Heterogenous late Holocene climate in the Eastern Mediterranean – the Kocain Cave record from SW Turkey

Matthew J. Jacobson[1, *], Pascal Flohr[1, 2], Alison Gascoigne[3], Melanie J. Leng[4, 5], Aleksey Sadekov[6], Hai Cheng[7, 8], R. Lawrence Edwards[9], Okan Tüysüz[10], Dominik Fleitmann[1, 11, *]

[1] School of Archaeology, Geography and Environmental Science, University of Reading, Reading, RG6 6UR, UK

[2] Cluster of Excellence ROOTS & Institute for Pre- and Protohistory, University of Kiel, Johanna-Mestorf Straße 2-6, 24118, Kiel, Germany

[3] Archaeology, University of Southampton, Southampton, SO17 1BJ, UK

[4] National Environmental Isotope Facility, British Geological Survey, Keyworth, NG12 5GG, UK

[5] School of Biosciences, University of Nottingham, Loughborough, LE12 5RD, UK

[6] Oceans Graduate School, Faculty of Engineering and Mathematical Sciences, University of Western Australia, Crawley, Perth, Western Australia 6009

[7] Institute of Global Environmental Change, Xi'an Jiatong University, Xi'an 710054, China

[8] Key Laboratory of Karst Dynamics, MLR, Institute of Karst Geology, CAGS, Guilin 541004, China

[9] Department of Earth and Environmental Sciences, University of Minnesota, Minneapolis, MN 55455, USA

[10] Eurasia Institute of Earth Sciences and Department of Geological Engineering, Istanbul Technical University, Istanbul, Turkey

[11] Department of Environmental Sciences, University of Basel, 4056 Basel, Switzerland

*Corresponding authors: Matthew J. Jacobson (m.j.jacobson2@pgr.reading.ac.uk)and Dominik Fleitmann (dominik.fleitmann@unibas.ch)

Key Points:

- Stalagmite Ko-1 record of effective-moisture from SW Turkey stresses spatial and temporal heterogeneity of Turkish climate
- Climate changes share more similarities with other Eastern Mediterranean coastal regions, than central or northern Turkey
- Heterogeneity of modern climate and proxy records highlight the complexity of historical comparisons

Abstract

Palaeoclimate variability must be constrained to predict the nature and impacts of future climate change in the Eastern Mediterranean. Here, we present a late Holocene high-resolution multiproxy dataset from Kocain Cave, the first of its kind from SW Turkey. Regional fluctuations in effective-moisture are recorded by variations in magnesium, strontium, phosphorous and carbon isotopes, with oxygen isotopes reacting to changes in precipitation and effective-moisture. The new record shows a double-peak of arid conditions at 1150 and 800 BCE, a wet period 330-460 CE followed by a rapid shift to dry conditions 460-830 CE, and a dry/wet Medieval Climate Anomaly/Little Ice Age pattern. Large discrepancies exist between Turkish records and the Kocain record, which shares more similarities with other Eastern Mediterranean coastal records. Heterogeneity of regional climate and palaeoclimate proxy records are emphasised.

Plain Language Summary

Records of past climate are essential in the Eastern Mediterranean to understand regional impacts of modern climate change. In combination with archaeology, these allow us to examine climatic impacts on people in the past to help us prepare for the future. Here, we examine a stalagmite (Ko-1) from Kocain Cave, southwest Turkey, which contains information about past climate change in its chemistry. Measurements of trace-metals and carbon isotope ratios record the amount of water entering the cave, oxygen isotope ratios record rainfall amount. Measurements of uraniuim are used to date the climate changes. Earthquakes that damaged nearby cities and caused tsunamis changed the angle of the stalagmite, providing more evidence for dating the sample.

The Kocain Cave record shows climatic conditions changed frequently in southwest Turkey. Important are dry conditions 1150 and 800 BCE, wet conditions 330-460 CE followed by a rapid shift to dry conditions 460-830 CE, and a dry/wet Medieval Climate Anomaly/Little Ice Age pattern. These climate changes were different to records from elsewhere in Turkey and matched better with coastal records from Greece and Lebanon/Israel. The complex nature of past climate is emphasised due to varied climatic regions in Turkey and the many impacts on each record.

1. Introduction

To predict the nature and impacts of future climate change in the Eastern Mediterranean (EM), a “hot-spot” which will experience severe impacts (Giorgi, 2006), past climatic variability must be constrained (Masson-Delmotte et al., 2013). Paucity of meteorological data (<100 years) renders palaeoclimate records vital for understanding spatio-temporal variance. Likewise, an abundance of archaeological data facilitates analysis of human-climate-environment interactions and resilience of past societies to climatic fluctuations (Luterbacher et al., 2012).

The climate of the EM is heterogenous over short distances (Ulbrich et al., 2012). Figure 1 shows spatial varitations in winter precipitation and Old World Drought Atlas (OWDA)-derived Palmer Drought Severity Index (PDSI) for two agricultural drought periods (Cook et al., 2015; University of East Anglia Climatic Research Unit et al., 2020), which are largely determined by effective-moisture. Agricultural droughts in (semi-)arid regions have a greater societal impact than individual climatic variables (Dalezios et al., 2017; Jones et al., 2019; Mannocchi et al., 2004). Confidently reconstructing this variability requires a dense network of precisely-dated and highly-resolved palaeoclimate records. Past spatio-temporal climate variability in the EM is, however, poorly documented due to unevenly distributed records (Burstyn et al., 2019; Luterbacher et al., 2012).

Figure 1: Late Holocene palaeoclimate archives (triangles) compared with CRU TS4.04 (University of East Anglia Climatic Research Unit et al., 2020) winter (Nov-Mar) precipitation and OWDA-derived PDSI (Cook et al., 2015) during agricultural drought periods (1580-1610 CE and 1980-2000 CE). Dotted square highlights Figure 2c. Data generated in the KNMI Climate Explorer (van Oldenborgh, 2020).

Extensive archaeological and pollen investigations (e.g. Vandam et al., 2019; Woodbridge et al., 2019) make SW Turkey a suitable testbed for examining human-climate-environment interactions. However, high-resolution palaeoclimate datasets from the region only extend back ~1000 (tree-rings) and ~1400 (Lake Salda) years (Danladi and Akçer-Ön, 2018; Heinrich et al., 2013), or do not cover the late Holocene (Dim Cave; Rowe et al., 2020; Ünal-İmer et al., 2016, 2015). Stable-isotopes from Lake Gölhisar (Eastwood et al., 2007) reveal low-resolution (~80 years) changes in lake water balance (LWB) throughout the Holocene, albeit with significant dating uncertainties of ±165 years. This record and tree-rings are seasonally biased towards spring/summer, whereas precipitation mainly occurs in winter (Peterson and Vose, 1997). High-resolution palaeoclimate archives are available from other regions of Turkey (Lake Nar, Sofular Cave; Dean et al., 2018; Göktürk et al., 2011); however, these are not local and experience wholly different climatic conditions (Section 5.1). Here, we provide a new speleothem record (Ko-1) from Kocain Cave, SW Turkey, to fill the late Holocene gap, We present highly-resolved trace-element (T-E) data starting ~950 BCE, and a stable-isotope record that extends from the present to ~1350 BCE. An age-model is constructed from uranium-series dates (^{230}Th), with supporting evidence from the impact of historically-attested earthquakes on Ko-1. This enables us to establish high-resolution climate variability in SW Turkey for >3000 years during the late Holocene.

2. Cave setting

Kocain Cave (37°13'57" N, 30°42'42" E; 730 m asl), western Taurus Mountains, formed within dolomitic Jurassic-Cenomanian shallow-marine limestones (Text S1, Figure S1; Demer et al., 2019) and is exceptionally large (opening width: 75m; gallery size: 36,000 m^2). Kocain has been utilised by humans since the Neolithic and contains a Roman spring-fed cistern, dated by early-Christian inscriptions (Talloen, 2015). Terrain above the cave is sparsely covered by typical C3-type Mediterranean vegetation, mainly evergreen shrubs (Koç et al., 2020).

Precipitation (1929-2018; Peterson & Vose, 1997) at Antalya exhibits a marked winter-peak, 90% occurring Nov-Mar, and high inter-annual variability, ranging from 207 mm (2008) to 1914 mm (1969). Alike the entire EM (Lionello, 2012; Xoplaki et al., 2018), SW Turkey experiences spatial heterogeneity of climate across short distances (Figure S2). Moisture is brought by westerly storm tracks (Ulbrich et al., 2012) and mountains promote orographic precipitation caused by rising moist air and associated rainout effects (Evans et al., 2004). Weather station data (Figure 2b) reveals that despite similar seasonal patterns, coastal stations (e.g. Antalya) are significantly warmer and wetter than inland stations (e.g. Isparta). Precipitation and temperature are enhanced during negative phases of the North-Sea Caspian Pattern (NCP), Arctic Oscillation (AO), and North Atlantic Oscillation (NAO), likely linked to increased cyclonic activity and circulation over the warm Mediterranean; however, these patterns are not the same across Turkey (Sariş et al., 2010; Unal et al., 2012; Section 5.1).

Figure 2: Conditions in the region surrounding Kocain cave. (**a**) Late Holocene palaeohydrological data with periods of high/low effective-moisture (green/brown shading), as indicated by original authors (Burdur, Gravgaz, Salda, Bereket) or deviations from the mean (Kocain, Gölhisar). The cistern terminus post quem (312 CE), soot layers (Koç et al., 2020), and dust-layer (335-485 CE) are displayed. (**b**) Average monthly precipitation (solid lines) and temperature (dashed lines) from weather stations in SW Turkey (Peterson & Vose, 1997). (**c**) Map of SW Turkey with late Holocene palaeoenvironmental archives (triangles) and weather stations (squares); colours correspond to stations in 2b.

3. Materials, Methodology and Chronology

The actively-growing stalagmite (Ko-1) from Kocain Cave, was collected ~450 m from the cave entrance in August 2005. Bedrock thickness above Ko-1 is ~80 m. A total of 31,503 measurements of T-Es (Ca, Mg, Sr, and P) were performed on the top 156 mm at a resolution of ~5 µm using Laser Ablation-Inductively Coupled Plasma-Mass Spectrometry (LA-ICP-MS) (Tanner et al., 2002). For oxygen ($\delta^{18}O$) and carbon ($\delta^{13}C$) isotope measurements, the first 174.5 mm was sampled at intervals of 0.5 mm or less, providing a total of 370 measurements. Further methodological description and sample extraction locations can be found in Text S2 and Figure S3.

For the chronology of Ko-1, 25 ^{230}Th ages were produced (following the analytical protocol of Cheng et al., 2013) ranging from 61±51 to 3387±80 BP (years before 1950 CE). Eight ages affected by significant detrital contamination ($^{230}Th/^{232}Th$ ratios <30) were not included in the age model (Figure 3b). The 17 remaining ^{230}Th ages have uncertainties varying from ±38-133 years (M=±67) and only one, at 43 mm depth, is not in stratigraphic order. Using these dates and the known collection date (August 2005), a *StalAge* age-model (Scholz and Hoffmann, 2011) was calculated.

Lateral shifts in the growth-axis at 457±100 CE (87.8 mm) and 176+30/-139 CE (110.3 mm) associated with historically-attested regional earthquakes provide additional evidence for the reliability of the constructed age-model. Tectonic activity altering the cave floor tilt is often a cause for speleothem growth-axis changes (Becker et al., 2006; Cadorin et al., 2001; Forti & Postpischl, 1984; Gilli, 2004; Gilli, 2005). For the ~457 CE displacement, earthquakes in 500, 518 and 528 CE were responsible for destruction of buildings in SW Turkey (Ergin et al., 1967; Gates, 1997; Malalas, 2017; Pirazzoli et al., 1996; Similox-Tohon et al., 2006; Stiros, 2001; Waelkens et al., 2000). The ~176 CE deviation is closely linked to an earthquake in 142 CE which caused extensive damage locally and a tsunami (Altinok et al., 2011; Ambraseys, 2009; Erel and Adatepe, 2007; Kokkinia, 2000; Papadopoulos et al., 2007; Tan et al., 2008). Further details of growth-axis deviations and speleoseismology can be found in Text S3 and Figure S5.

4. Interpretation of the Ko-1 multi-proxy record

$\delta^{13}C$ and $\delta^{18}O$ values from Ko-1 were previously interpreted as reflecting changes in winter temperature and associated snow melt (Göktürk, 2011). New T-E measurements (Figure 3) disprove this interpretation, indicating variations in the multi-proxy record can be used to characterise regional fluctuations in effective-moisture (Mg/Ca, Sr/Ca), effective-moisture/biological activity (P/Ca, $\delta^{13}C$), and effective-moisture/precipitation amount ($\delta^{18}O$).

All Ko-1 proxy records correlate and are visually similar as all are influenced to various extents by changes in effective-moisture (Figures 3a and S6). Prior calcite precipitation (PCP) occurs when cave drip-waters reach a gas phase above the cave with lower partial pressure of carbon dioxide (pCO_2) than the soil gas CO_2 with which they were previously in equilibrium (McDonald et al., 2004). This enhances Mg/Ca, Sr/Ca, and $\delta^{13}C$ ratios, as Ca^{2+} and ^{12}C are preferentially deposited (Fohlmeister et al., 2020; McDermott et al., 2006). Additional PCP occurs in periods of low effective-moisture as there are more aerated spaces above the cave and longer aquifer interaction times (Fairchild and Treble, 2009; Treble et al., 2003; Tremaine and Froelich, 2013). A positive correlation between Mg/Ca and Sr/Ca ($r=0.57$, $p<0.0001$) provides evidence for PCP (Wassenburg et al., 2020). During drier intervals, longer groundwater residence times will enhance Mg/Ca further, but not Sr/Ca, due to dissolution of the overlying dolomitic limestones (Fairchild and Treble, 2009).

Increased effective-moisture enhances vegetation cover, soil microbial activity and drip-rates, and causes the ratio between C_3 and C_4 plants to increase (Cheng et al., 2015; Genty et al., 2001). C_4 plants are adapted to warm and (semi-)arid climates and have ~14‰ less negative $\delta^{13}C$ than C_3 plants (Farquhar, 1983; Farquhar et al., 1989; Henderson et al., 1992). Increased biological activity depletes stalagmite $\delta^{13}C$ values and releases bio-available P that is transported during intense soil infiltration (Fairchild et al., 2007, 2001; Treble et al., 2003). The influence of effective-moisture on P/Ca ratios is supported by strong negative correlations with Mg/Ca ($r=-0.60$, $p<0.0001$) and Sr/Ca ($r=-0.87$, $p<0.0001$). A positive correlation between $\delta^{18}O$ and $\delta^{13}C$ ($r=0.47$, $p<0.0001$) provides evidence for kinetic fractionation, likely related to fluctuations in drip-rate (Hendy, 1971). However, the interpretation of $\delta^{18}O$ in Ko-1 is complicated, as with other Turkish speleothems (see Fleitmann et al., 2009; Göktürk, 2011). Global Network of Isotopes in Precipitation (GNIP) data from Antalya (Figure S8; IAEA/WMO, 2021) show a negative correlation between $\delta^{18}O$ and precipitation ($r=-0.30$, $p<0.0001$; "the amount effect"; Dansgaard, 1964), and a stronger correlation with temperature ($r=0.44$, $p<0.0001$). Precipitation seasonality will also alter $\delta^{18}O$, with isotopically-lighter $\delta^{18}O$ precipitated in winter (Nov-Mar; M=–5.6 ‰, SD=2.1) compared to summer (Jun-Aug; M=–3.4 ‰, SD=2.6). In Ko-1, more negative $\delta^{18}O$ coincides with lower Mg/Ca (Figure 3), this relationship can be explained by the importance of precipitation (and temperature) in determining effective-moisture (Sinha et al., 2019).

Furthermore, agreement between high magnitude changes in the Ko-1 proxies, and other regional proxies, suggest they reflect effective-moisture (Figures 2 and 4; Section 6). Most notable is a distinct phase of high effective-moisture (330-460 CE), near-contemporaneous with a distinct brown/orange dust-layer on Ko-1 (87.3-98 mm; 335-485 CE), containing a soot layer (Koç et al., 2020), and cistern construction in Kocain Cave (Figure 2). A prominent labarum/*Chi-Rho* symbol (☧) gives this cistern (~250 m^3 capacity) a 312 CE *terminus post quem* (earliest possible construction date), as that is when it was incorporated as a shield emblem by Emperor Constantine (Cameron and Hall, 1999), its use remained extensive until the 6th century CE

(Hörandner and Carr, 2005). During numerous visits to the cave by the authors between Aug. 2005 and Apr. 2019, this cistern was 0-10% full (0-25 m^3) and spring flow was occurring but minimal. We suggest it was built during a period of greater spring flow and this, combined with the caves large opening width, made it suitable for use by herders. This assumption is further supported by a regional increase in grazing during the Late Roman Period (300-450 CE), specifically a shift towards goat herding in "marginal" mountainside areas (De Cupere et al., 2017; Fuller et al., 2012; Izdebski, 2012; Poblome, 2015). Animal herds' use of the cistern would have mobilised fine dust from the cave floor, which was then incorporated into the stalagmite. High Fe/Ca ratios are detected in this layer, suggesting dust particles were trapped as it was precipitated (Fairchild and Treble, 2009; Figure S4). This mechanism could explain the dust-layer; which would usually suggest drier conditions if corresponding to increases in Mg/Ca (see Carolin et al., 2019).

High effective-moisture in the 4th and early 5th centuries CE is also evidenced by wild weeds that require high moisture availability growing in the territory of Sagalassos (Bakker et al., 2012; Kaniewski et al., 2007); wetland conditions and spring reactivation in the Bereket Valley and Gravgaz Marsh (Bakker et al., 2013; Kaptijn et al., 2013; Van Geel et al., 1989; Vermoere et al., 2002); and deep-water conditions at Lake Burdur (Tudryn et al., 2013). Similar changes are evidenced in EM proxies, suggesting this wet phase was a regional phenomenon (see below). The above interpretations, and corroborating evidence, strengthen our claim that decreases in Ko-1 Mg/Ca, Sr/Ca, $\delta^{13}C$ and $\delta^{18}O$, with increases in P/Ca, are indicative of wetter climatic conditions in SW Turkey.

5. Ko-1 Record and EM Palaeoclimate

Key palaeohydrological changes for SW Turkey are reflected in geochemical proxies in Ko-1 (Figures 3, S7). First, distinct phases of low effective-moisture are centred at ~1150 and ~800 BCE, with intervening wetter conditions between ~1000 and 900 BCE. Secondly, high effective-moisture occurred between ~330 and 460 CE, followed by a rapid shift to drier conditions that lasted until ~830 CE. Finally, there was a dry/wet Medieval Climate Anomaly (MCA; 850-1300 CE)/Little Ice Age (LIA; 1400-1700 CE) pattern, with high variability during 1450-1550 CE.

Figure 3: Stable-isotope (‰) and trace-element ($mmol/mol^{-1}$) palaeoclimate proxy records from Kocain Cave. (**a**) Ko-1 proxies aligned so peaks represent wetter conditions. Trace-elements are displayed as annual (grey) and 15-year (colours) averages. (**b**) *StalAge* model for Ko-1. Earthquakes were not input to the model. (**c**) Comparison between Mg/Ca and $\delta^{18}O$ ratios. Blue line represents the mean value of both records ($0.88 mmol/mol^{-1}$ and –3.76‰).

Marked palaeohydrological changes between 1200 and 750 BCE are widespread and often associated with cold phases, such as the 3.2 and 2.8 ka events and Crisis Years Cooling Event (CYCE), and reductions in solar irradiance (Kaniewski et al., 2019; Mayewski et al., 2004; Steinhilber et al., 2009; Wanner et al., 2015). Links between these changes and socio-political change remain controversial (Drake, 2012; Finné et al., 2017; Kaniewski et al., 2013; Knapp and Manning, 2016; Manning et al., 2020). While similar palaeohydrological changes to those revealed by Ko-1 are observed in records such as Gölhisar, Skala Marion, and Tell Tweini (Eastwood et al., 2007; Kaniewski et al., 2019; Psomiadis et al., 2018), others are dissimilar

(Figure 4). No aridification is observed at Sofular, Nar, or Tecer (Dean et al., 2018; Fleitmann et al., 2009; Göktürk et al., 2011; Jones et al., 2006; Kuzucuoğlu et al., 2011), whereas a single shift to more arid conditions is evidenced at Iznik, Van, Mavri Trypa, Jeita, Soreq, and in the Middle East in general (Bar-Matthews et al., 2003; Barlas Şimşek and Çağatay, 2018; Cheng et al., 2015; Finné et al., 2017; Sinha et al., 2019; Ülgen et al., 2012).

Wet conditions between ~330 and 460 CE rapidly shift to an arid phase between ~460 and 830 CE in the Ko-1 record, roughly coincident with the Dark Ages Cold Period (DACP: 450-800 CE; Helama et al., 2017; Figure 4). An effective-moisture peak in SW Turkey is supported by local palaeoenvironmental evidence and archaeological evidence in Kocain Cave (see above). Similar wet peaks are observed across the EM at ~300-500 CE. Speleothem $\delta^{18}O$ data from Mavri Trypa and Skala Marion caves demonstrate wet conditions at ~300-350 CE (Finné et al., 2017; Psomiadis et al., 2018). Effective-moisture proxies from Lake Trichonida show an apparently delayed response, with the records wettest phase between ~420 and 500 CE (Seguin et al., 2020). Reconstructed precipitation based on Dead Sea data suggests ~350-490 CE may be the wettest interval in the late Holocene for the southern Levant, whereas a depletion of isotopes from Jeita Cave suggests a break from arid conditions between ~320 and 400 CE (Cheng et al., 2015; Morin et al., 2019).

Generally, these wet phases are followed by a rapid shift to drier conditions in the 5th century (Figure 4). This pre-dates the Late Antique Little Ice Age (LALIA)/"536-550 CE climate downturn" (Büntgen et al., 2016; Newfield, 2018), a phasing that is also observed in records from the Middle East (e.g. Sharifi et al., 2015). However, other Turkish records show very different palaeohydrological changes. Locally, wet conditions prevailed longer: high detrital and low carbonate content at the start of the Lake Salda record (~550-600 CE) indicate wet conditions, cluster analysis of pollen and non-pollen palynomorphs from Gravgaz Marsh reveal wet conditions until 640 CE, and $\delta^{18}O$ data from Gölhisar remains depleted until ~800 CE (Bakker et al., 2011; Danladi & Akçer-Ön, 2018; Eastwood et al., 2007). Records from northern (Sofular), central (Nar, Tecer) and eastern (Van) Turkey show the inverse to Ko-1, with a marked dry phase starting ~300-350 CE, followed by a shift to humid conditions at ~500-550 CE that endured for centuries (Barlas Şimşek and Çağatay, 2018; Dean et al., 2018; Fleitmann et al., 2009; Kuzucuoğlu et al., 2011).

Enhanced variation in effective-moisture is evidenced in the Ko-1 record from ~800 until 1850 CE (Figures 3 and 4). From ~900 CE until ~1460 CE, drier conditions prevailed, with more-humid intervals every ~120-150 years (~1030, ~1180, ~1300 CE), encompassing the MCA. Hydroclimate was highly variable between ~1450 and 1550 CE, experiencing an extreme dry-wet-dry-wet pattern. The driest conditions in the entire Ko-1 record occur between 1510-1530 CE, indicated by the highest $\delta^{18}O$ value and 15-year Mg/Ca and P/Ca averages. Subsequently, effective-moisture was still highly variable but elevated until ~1840 CE, a period roughly coincident with the LIA (1400-1850 CE). Reconstructed winter-spring temperatures from tree-rings in Jsibeli suggest cooling after ~1500 CE, with the coldest conditions at ~1750 CE (Heinrich et al., 2013), when there was a break from high effective-moisture at Kocain (Figure 4).

The dry/wet MCA/LIA pattern observed at Kocain Cave contrasts with other records from Turkey (Burdur, Salda, Nar, Sofular, Iznik), which show the inverse pattern (Danladi and Akçer-Ön, 2018; Dean et al., 2015; Fleitmann et al., 2009; Tudryn et al., 2013; Ülgen et al., 2012), and from the Fertile Crescent (Jeita, Kfar Giladi, Soreq, Gejkar, Neor), which show no pattern (Bar-Matthews et al., 2003; Cheng et al., 2015; Flohr et al., 2017; Luterbacher et al., 2012; Morin et al., 2019; Sharifi et al., 2015; Figures 4 and S9). Most high-resolution Greek/Aegean records do not cover this more recent time interval. However, Trichonida log(Rb/Sr) exhibits strong similarities to Ko-1 (Figure 4). Dry conditions ~900-1450 CE follow a wetter phase ~850 CE, with breaks at 1050 and 1300 CE. Increased effective-moisture is then demonstrated until 1650 CE, before another peak in the early 19th century CE, also evidenced in Nar diatom $\delta^{18}O$ (Dean et al., 2018; Seguin et al., 2020).

Figure 4: Late Holocene EM palaeoclimate data compared with Ko-1 Mg/Ca (15-year averages) and $\delta^{18}O$ (‰VPDB). Peaks in all records (excl. Jsibeli) indicate wetter conditions. Warm/cold intervals are: Crisis Years Cold Event (CYCE), Roman Climatic Optimum (RCO), Dark Ages Cold Period (DACP), Medieval Climate Anomaly (MCA), and Little Ice Age (LIA). For references, see text.

5.1. Heterogeneity of Eastern Mediterranean climate and proxies

Large discrepancies exist between the Ko-1 record of effective-moisture and other hydrological proxies from the EM, most likely caused by: (1) spatial climate variations and challenges in palaeoclimate analysis, related to (2) interpretation of different types of proxies with varied sensitivity to hydroclimatic change and (3) chronological uncertainties. The greatest differences between records discussed here are observed between Ko-1 and other records from Turkey. Climatic heterogeneity in SW Turkey is more extreme across the large country (780,000 km^2), which has complex and diverse topography, and numerous moisture sources (Lionello, 2012; Xoplaki et al., 2018). These factors lead to varied temperatures (Aydın et al., 2019), seasonal patterns (Sariş et al., 2010), and impacts from teleconnections (Ünal-İmer et al., 2015; Unal et al., 2012).

The two other high-resolution Turkish records that contrast with Ko-1, Lake Nar (central Anatolian plateau: CAP) and Sofular Cave (NW Turkey; Black Sea coast), are in completely different climatic regions. The high elevation CAP region experiences low precipitation (m=455 mm/yr^{-1}), with two peaks (Apr.-May/Oct.-Dec.), and cold semi-arid and dry continental climates (Öztürk et al., 2017; Peel et al., 2007). The Black Sea coast is temperate, with precipitation of a similar magnitude to SW Turkey (m=915 mm/yr^{-1}), but there is no dry season and precipitation is high throughout the year (Göktürk et al., 2011, 2008; Karaca et al., 2000). The impact of large-scale atmospheric teleconnections (NCP, AO, NAO) also differs in these regions, compared to SW Turkey which has enhanced precipitation and temperature during negative phases (Kutiel et al., 2002; Sezen and Partal, 2019). Negative phases cause higher temperatures across Turkey, particularly in winter. However, the CAP experiences significantly greater increases (Kutiel and Türkeş, 2005; Türkeş and Erlat, 2009). Impacts on precipitation are more varied. The Black Sea weakens the impacts of teleconnections on precipitation in NW Turkey (Göktürk et al., 2011; Türkeş and Erlat, 2003). AO- and NCP- phases cause their most significant impact on precipitation in SW Turkey (Kutiel and Benaroch, 2002), with CAP only impacted by AO- phases in winter (Sezen and Partal, 2019) and the transition between enhancements/reductions in precipitation from NCP- phases located <50 km from Nar (Kutiel et al., 2002; Kutiel and Türkeş, 2005). NAO influence is weaker and focused on the western and central regions (Unal et al., 2012). These differences lead to spatial variations in droughts, which impact each record differently (Figures 1 and S10; Vicente-Serrano et al., 2010). Lake Nar records LWB, with higher $\delta^{18}O$ corresponding to hydrological droughts (lake-water deficits) (Jones et al., 2019). Speleothems record fluctuations in EM, which are more akin to agricultural droughts (soil-moisture availability) (Fleitmann et al., 2009; Göktürk et al., 2011). However, none of these records are simple, being influenced by multiple climatic and geological/geographical factors, the importance of which changes over time. Additionally, proxies represent different seasons. The carbonate $\delta^{18}O$ record from Lake Nar is primarily deposited in early summer in response to evaporation and aridity (Dean et al., 2015). Speleothem records are winter-season biased due to the lighter-isotopic signature of winter precipitation and seasonality of precipitation (e.g. in SW Turkey).

The impact of temperature change on precipitation and proxy records is also poorly understood and variable. Antalya GNIP data shows a negative correlation between precipitation and temperature ($r=-0.53$, $p<0.0001$; Figure S8). However, proxy records show both increases and decreases in effective-moisture during periods with lower temperatures: during the CYCE effective-moisture is low, but during the LIA effective-moisture is high at Kocain Cave (Figure 4).

Comparison between records is further complicated by chronological uncertainties of decadal-centurial length in lake and speleothem records. Multiple and varied lags are present between climatic changes in different regions, and between climatic shifts and their signal in records. Different resolutions hinder comparison and the specifics of resolutions, i.e., whether a sample is an average across a large period or a specific point in time, are rarely addressed.

6. Conclusion

Stalagmite Ko-1, from Kocain Cave, provides the first highly-resolved, well-dated palaeohydrological proxy record covering the late Holocene for SW Turkey. Key periods of palaeoclimatic change are revealed, notably: (1) a double-peak of arid conditions (1150 and 800 BCE), (2) a distinct period of high effective-moisture in the 4^{th} and 5^{th} centuries CE (~330 to 460 CE), followed by (3) a rapid shift to low effective-moisture (460 CE) that persisted until ~830 CE, and finally (4) a dry/wet MCA/LIA pattern. Changes were often in contrast to palaeoclimate records from northern and central Turkey, and sometimes locally, more frequently correlating with changes in coastal records from the Aegean and Levant regions. Considering the heterogeneity of climate and the multitude of impacts on records, palaeoclimatic interpretations are complex and care must be taken especially when they are utilised for discussions of societal impacts.

Acknowledgments, Samples, and Data

The new Kocain speleothem (Ko-1) uranium-series, trace-element and stable-isotope data used in this study are available from the NOAA palaeoclimate archive via https://www.ncdc.noaa.gov/paleo/study/33854 and in the supporting information. This work was supported by the AHRC South, West and Wales Doctoral Training Partnership (Grant AH/L503939/1 to MJJ), the Swiss National Science Foundation (Grant PP002-110554/1 to DF), the U.S. National Science Foundation (Grant 1702816 to RLE), the ERC Advanced Grant (2010 NEWLOG ADG-267931 to AS, awarded to Prof. H. Elderfield) and the National Natural

Science Foundation of China (Grant NSFC 41888101 to HC). The isotope and trace-element data were provided by the National Environmental Isotope Facility and the Department of Earth Science, University of Cambridge, respectively. We would also like to thank Dr. Mark Lütscher for his support during the 2005 field trip when the Ko-1 sample was collected.

References

Altinok, Y., Alpar, B., Özer, N., Aykurt, H., 2011. Revision of the tsunami catalogue affecting Turkish coasts and surrounding regions. Nat. Hazards Earth Syst. Sci. 11, 273–291. https://doi.org/10.5194/nhess-11-273-2011

Ambraseys, N., 2009. Earthquakes in the eastern Mediterranean and the Middle East: a multidisciplinary study of 2000 years of seismicity. Cambridge University Press, Cambridge.

Aydın, S., Şimşek, M., Çetinkaya, G., Öztürk, M.Z., 2019. Erinç Yağış Etkinlik İndisi'ne Göre Belirlenen Türkiye İklim Bölgelerinin Rejim Karakteristikleri (Regime Characteristiscs of Turkey's Climatic Regions Determined Using the Erinç Precipitation Efficiency Index), in: 1st Istanbul International Geography Congress Proceedings Books. Istanbul University Press, Istanbul, pp. 752–760. https://doi.org/10.26650/PB/PS12.2019.002.074

Bakker, J., Kaniewski, D., Verstraeten, G., De Laet, V., Waelkens, M., 2011. Numerically derived evidence for late-Holocene climate change and its impact on human presence in the southest Taurus Mountains, Turkey. Holocene 22, 425–438. https://doi.org/10.1177/0959683611425546

Bakker, J., Paulissen, E., Kaniewski, D., de Laet, V., Verstraeten, G., Waelkens, M., 2012. Man, vegetation and climate during the Holocene in the territory of Sagalassos, Western Taurus Mountains, SW Turkey. Veg. Hist. Archaeobot. 21, 249–266. https://doi.org/10.1007/s00334-011-0312-4

Bakker, J., Paulissen, E., Kaniewski, D., Poblome, J., De Laet, V., Verstraeten, G., Waelkens, M., 2013. Climate, people, fire and vegetation: New insights into vegetation dynamics in the Eastern Mediterranean since the 1st century AD. Clim. Past 9, 57–87. https://doi.org/10.5194/cp-9-57-2013

Bar-Matthews, M., Ayalon, A., Gilmour, M., Matthews, A., Hawkesworth, C.J., 2003. Sea–land oxygen isotopic relationships from planktonic foraminifera and speleothems in the Eastern Mediterranean region and their implication for paleorainfall during interglacial intervals. Geochim. Cosmochim. Acta 67, 3181–3199.

Barlas Şimşek, F., Çağatay, M.N., 2018. Late Holocene high resolution multi-proxy climate and environmental records from Lake Van, eastern Turkey. Quat. Int. 486, 57–72. https://doi.org/10.1016/j.quaint.2017.12.043

Becker, A., Davenport, C.A., Eichenberger, U., Gilli, E., Jeannin, P.Y., Lacave, C., 2006. Speleoseismology: A critical perspective. J. Seismol. 10, 371–388. https://doi.org/10.1007/s10950-006-9017-z

Büntgen, U., Myglan, V.S., Ljungqvist, F.C., McCormick, M., Di Cosmo, N., Sigl, M., Jungclaus, J., Wagner, S., Krusic, P.J., Esper, J., Kaplan, J.O., De Vaan, M.A.C., Luterbacher, J., Wacker, L., Tegel, W., Kirdyanov, A. V., 2016. Cooling and societal change during the Late Antique Little Ice Age from 536 to around 660 AD. Nat. Geosci. 9, 231–236. https://doi.org/10.1038/ngeo2652

Burstyn, Y., Martrat, B., Lopez, Jordi, F., Iriarte, E., Jacobson, M.J., Lone, M.A., Deininger, M., 2019. Speleothems from the Middle East: An Example of Water Limited Environments in the SISAL Database. Quaternary 2. https://doi.org/10.3390/quat2020016

Cadorin, J.F., Jongmans, D., Plumier, A., Camelbeeck, T., Delaby, S., Quinif, Y., 2001. Modelling of speleothems failure in the Hotton cave (Belgium). Is the failure earthquake induced? Netherlands J. Geosci. 80, 315–321. https://doi.org/10.1017/S001677460002391X

Cameron, A., Hall, S., 1999. Eusebius of Caesarea: Vita Constantini (Life of Constantine). Oxford University Press, New York.

Carolin, S.A., Walker, R.T., Day, C.C., Ersek, V., Alastair Sloan, R., Dee, M.W., Talebian, M., Henderson, G.M., 2019. Precise timing of abrupt increase in dust activity in the Middle East coincident with 4.2 ka social change. Proc. Natl. Acad. Sci. U. S. A. 116, 67–72. https://doi.org/10.1073/pnas.1808103115

Cheng, H., Lawrence Edwards, R., Shen, C.C., Polyak, V.J., Asmerom, Y., Woodhead, J., Hellstrom, J., Wang, Y., Kong, X., Spötl, C., Wang, X., Calvin Alexander, E., 2013. Improvements in 230 Th dating, 230 Th and 234 U half-life values, and U-Th isotopic measurements by multi-collector inductively coupled plasma mass spectrometry. Earth Planet. Sci. Lett. 371–372, 82–91. https://doi.org/10.1016/j.epsl.2013.04.006

Cheng, H., Sinha, A., Verheyden, S., Nader, F.H., Li, X.L., Zhang, P.Z., Yin, J.J., Yi, L., Peng, Y.B., Rao, Z.G., Ning, Y.F., Edwards, R.L., 2015. The climate variability in northern Levant over the past 20,000 years. Geophys. Res. Lett. 42, 8641–8650. https://doi.org/10.1002/2015GL065397

Cook, E.R., Seager, R., Kushnir, Y., Briffa, K.R., Büntgen, U., Frank, D., Krusic, P.J., Tegel, W., van der Schrier, G., Andreu-Hayles, L., Baillie, M., Baittinger, C., Bleicher, N., Bonde, N., Brown, D., Carrer, M., Cooper, R., Čufar, K., Dittmar, C., Esper, J., Griggs, C., Gunnarson, B., Günther, B., Gutierrez, E., Haneca, K., Helama, S., Herzig, F., Heussner, K.-U., Hofmann, J., Janda, P., Kontic, R., Köse, N., Kyncl, T., Levanič, T., Linderholm, H., Manning, S., Melvin, T.M., Miles, D., Neuwirth, B., Nicolussi, K., Nola, P., Panayotov, M., Popa, I., Rothe, A., Seftigen, K., Seim, A., Svarva, H., Svoboda, M., Thun, T., Timonen, M., Touchan, R., Trotsiuk, V., Trouet, V., Walder, F., Ważny, T., Wilson, R., Zang, C., 2015. Old World megadroughts and pluvials during the Common Era. Sci. Adv. 1, e1500561. https://doi.org/10.1126/sciadv.1500561

Dalezios, N.R., Gobin, A., Tarquis Alfonso, A.M., Eslamian, S., 2017. Agricultural Drought Indices: Combining Crop, Climate, and Soil Factors, in: Eslamian, S., Eslamian, F. (Eds.), Handbook of Drought and Water Scarcity: Environmental Impacts and Analysis of Drought and Water Scarcity. CRC Press, Boca Raton, pp. 73–89. https://doi.org/10.1201/9781315404219-5

Danladi, I.B., Akçer-Ön, S., 2018. Solar forcing and climate variability during the past millennium as recorded in a high altitude lake: Lake Salda (SW Anatolia). Quat. Int. 486, 185–198. https://doi.org/10.1016/j.quaint.2017.08.068

Dansgaard, W., 1964. Stable isotopes in precipitation. Tellus 16, 436–468. https://doi.org/10.3402/tellusa.v16i4.8993

De Cupere, B., Frémondeau, D., Kaptijn, E., Marinova, E., Poblome, J., Vandam, R., Van Neer, W., 2017. Subsistence economy and land use strategies in the Burdur province (SW Anatolia) from prehistory to the Byzantine period. Quat. Int. 436, 4–17. https://doi.org/10.1016/j.quaint.2015.11.097

Dean, J.R., Jones, M.D., Leng, M.J., Metcalfe, S.E., Sloane, H.J., Eastwood, W.J., Roberts, C.N., 2018. Seasonality of Holocene hydroclimate in the Eastern Mediterranean reconstructed using the oxygen isotope composition of carbonates and diatoms from Lake Nar, central Turkey. Holocene 28, 267–276. https://doi.org/10.1177/0959683617721326

Dean, J.R., Jones, M.D., Leng, M.J., Noble, S.R., Metcalfe, S.E., Sloane, H.J., Sahy, D., Eastwood, W.J., Roberts, C.N., 2015. Eastern Mediterranean hydroclimate over the late glacial and Holocene, reconstructed from the sediments of Nar lake, central Turkey, using stable isotopes and carbonate mineralogy. Quat. Sci. Rev. 124, 162–174. https://doi.org/10.1016/j.quascirev.2015.07.023

Demer, S., Elitok, Ö., Memiş, Ü., 2019. Origin and geochemical evolution of groundwaters at the northeastern extend of the active Fethiye-Burdur fault zone within the ophiolitic Teke nappes, SW Turkey. Arab. J. Geosci. 12. https://doi.org/10.1007/s12517-019-4963-2

Drake, B.L., 2012. The influence of climatic change on the Late Bronze Age Collapse and the Greek Dark Ages. J. Archaeol. Sci. 39, 1862–1870. https://doi.org/10.1016/j.jas.2012.01.029

Eastwood, W.J., Leng, M.J., Roberts, N., Davis, B., 2007. Holocene climate change in the eastern Mediterranean region: A comparison of stable isotope and pollen data from Lake Gölhisar, southwest Turkey. J. Quat. Sci. 22, 327–341. https://doi.org/10.1002/jqs.1062

Erel, T., Adatepe, F., 2007. Traces of historical earthquakes in the ancient city life at the Mediterranean region. J. Black Sea / Mediterr. Environ. 13, 241–252.

Ergin, K., Guclu, U., Uz, Z., 1967. A Catalog of Earthquakes for Turkey and the Surrounding Area (11 A.D. to 1964 A.D.). Istanbul Technical Univeristy, Istanbul.

Evans, J.P., Smith, R.B., Oglesby, R.J., 2004. Middle East climate simulation and dominant precipitation processes. Int. J. Climatol. 24, 1671–1694. https://doi.org/10.1002/joc.1084

Fairchild, I.J., Baker, A., Borsato, A., Frisia, S., Hinton, R.W., McDermott, F., Tooth, A.F., 2001. Annual to sub-annual resolution of multiple trace-element trends in speleothems. J. Geol. Soc. London. 158, 831–841. https://doi.org/10.1144/jgs.158.5.831

Fairchild, I.J., Frisia, S., Borsato, A., Tooth, A.F., 2007. Speleothems, in: Nash, D.J., McLaren, S.J. (Eds.), Geochemical Sediments and Landscapes. Blackwell Publishing Ltd, Oxford, pp. 200–245.

Fairchild, I.J., Treble, P.C., 2009. Trace elements in speleothems as recorders of environmental change. Quat. Sci. Rev. 28, 449–468. https://doi.org/10.1016/j.quascirev.2008.11.007

Farquhar, G.D., 1983. On the Nature of Carbon Isotope Discrimination in C4 Species. Aust. J. Plant Physiol. 10, 205–226.

Farquhar, G.D., Ehleringer, J.R., Hubick, K.T., 1989. Carbon Isotope Discrimination and Photosynthesis. Annu. Rev. Plant Physiol. Plant Mol. Biol. 40, 503–537.

Finné, M., Holmgren, K., Shen, C.C., Hu, H.M., Boyd, M., Stocker, S., 2017. Late Bronze Age climate change and the destruction of the Mycenaean palace of Nestor at Pylos. PLoS One 12, e0189447. https://doi.org/10.1371/journal.pone.0189447

Fleitmann, D., Cheng, H., Badertscher, S., Edwards, R.L., Mudelsee, M., Göktürk, O.M., Fankhauser, A., Pickering, R., Raible, C.C., Matter, A., Kramers, J., Tüysüz, O., 2009. Timing and climatic impact of Greenland interstadials recorded in stalagmites from northern Turkey. Geophys. Res. Lett. 36, 1–5. https://doi.org/10.1029/2009GL040050

Flohr, P., Fleitmann, D., Zorita, E., Sadekov, A., Cheng, H., Bosomworth, M., Edwards, L., Matthews, W., Matthews, R., 2017. Late Holocene droughts in the Fertile Crescent recorded in a speleothem from northern Iraq. Geophys. Res. Lett. 44, 1528–1536. https://doi.org/10.1002/2016GL071786

Fohlmeister, J., Voarintsoa, N.R.G., Lechleitner, F.A., Boyd, M., Brandtstätter, S., Jacobson, M.J., Oster, J.L., 2020. Main controls on the stable carbon isotope composition of speleothems. Geochim. Cosmochim. Acta 279, 67–87. https://doi.org/10.1016/j.gca.2020.03.042

Forti, P., Postpischl, D., 1984. Seismotectonic and paleoseismic analyses using karst sediments. Mar. Geol. 55, 145–161. https://doi.org/10.1016/0025-3227(84)90138-5

Fuller, B.T., De Cupere, B., Marinova, E., Van Neer, W., Waelkens, M., Richards, M.P., 2012. Isotopic reconstruction of human diet and animal husbandry practices during the Classical-Hellenistic, imperial, and Byzantine periods at Sagalassos, Turkey. Am. J. Phys. Anthropol. 149, 157–171. https://doi.org/10.1002/ajpa.22100

Gates, M.-H., 1997. Archaeology in Turkey. Am. J. Archaeol. 101, 241. https://doi.org/10.2307/506511

Genty, D., Baker, A., Massault, M., Proctor, C., Gilmour, M., Pons-Branchu, E., Hamelin, B., 2001. Dead carbon in stalagmites: Carbonate bedrock paleodissolution vs. ageing of soil organic matter. Implications for 13C variations in speleotherms. Geochim. Cosmochim. Acta 65, 3443–3457. https://doi.org/10.1016/S0016-7037(01)00697-4

Gilli, É., 2005. Point sur l'utilisation des spéléothèmes comme indicateurs de paléosismicité ou de néotectonique. Comptes Rendus - Geosci. 337, 1208–1215. https://doi.org/10.1016/j.crte.2005.05.008

Gilli, É., 2004. Glacial causes of damage and difficulties to use speleothems as palaeoseismic indicators. Geodin. Acta 17, 229–240. https://doi.org/10.3166/ga.17.229-240

Giorgi, F., 2006. Climate change hot-spots. Geophys. Res. Lett. 33, 1–4. https://doi.org/10.1029/2006GL025734

Göktürk, O.M., 2011. Climate in the Eastern Mediterranean through the Holocene inferred from Turkish stalagmites (PhD Thesis). University of Bern, Switzerland.

Göktürk, O.M., Bozkurt, D., Şen, Ö.L., Karaca, M., 2008. Quality control and homogeneity of Turkish precipitation data. Hydrol. Process. 22, 3210–3218. https://doi.org/10.1002/HYP.6915

Göktürk, O.M., Fleitmann, D., Badertscher, S., Cheng, H., Edwards, R.L., Leuenberger, M., Fankhauser, A., Tüysüz, O., Kramers, J., 2011. Climate on the southern Black Sea coast during the Holocene: Implications from the Sofular Cave record. Quat. Sci. Rev. 30, 2433–2445. https://doi.org/10.1016/j.quascirev.2011.05.007

Heinrich, I., Touchan, R., Dorado Liñán, I., Vos, H., Helle, G., 2013. Winter-to-spring temperature dynamics in Turkey derived from tree rings since AD 1125. Clim. Dyn. 41, 1685–1701. https://doi.org/10.1007/s00382-013-1702-3

Helama, S., Jones, P.D., Briffa, K.R., 2017. Dark Ages Cold Period: A literature review and directions for future research. Holocene. https://doi.org/10.1177/0959683617693898

Henderson, S.A., von Caemmerer, S., Farquhar, G.D., 1992. Short-term Measurements of Carbon Isotope Discrimination in Several C4 Species. Aust. J. Plant Physiol. 19, 263–285.

Hendy, C.H., 1971. The isotopic geochemistry of speleothems-I. The calculation of the effects of different modes of formation on the isotopic composition of speleothems and their applicability as palaeoclimatic indicators. Geochim. Cosmochim. Acta 35, 801–824. https://doi.org/10.1016/0016-7037(71)90127-X

Hörandner, W., Carr, A.W., 2005. Chi Rho, in: Kazhdan, A.P. (Ed.), The Oxford Dictionary of Byzantium. Oxford University Press, Oxford.

IAEA/WMO, 2021. Global Network of Isotopes in Precipitation [WWW Document]. URL http://www.iaea.org/water (accessed 7.17.20).

Izdebski, A., 2012. A rural world in transition: Asia Minor from Late Antiquity into the early Middle Ages. Taubenschlag Foundation, Berlin.

Jones, M.D., Abu-Jaber, N., AlShdaifat, A., Baird, D., Cook, B.I., Cuthbert, M.O., Dean, J.R., Djamali, M., Eastwood, W., Fleitmann, D., Haywood, A., Kwiecien, O., Larsen, J., Maher, L.A., Metcalfe, S.E., Parker, A., Petrie, C.A., Primmer, N., Richter, T., Roberts, N., Roe, J., Tindall, J.C., Ünal-İmer, E., Weeks, L., 2019. 20,000 years of societal vulnerability and adaptation to climate change in southwest Asia. Wiley Interdiscip. Rev. Water 6, e1330. https://doi.org/10.1002/wat2.1330

Jones, M.D., Roberts, C.N., Leng, M.J., Türkeş, M., 2006. A high-resolution late Holocene lake isotope record from Turkey and links to North Atlantic and monsoon climate. Geology 34, 361–364. https://doi.org/10.1130/G22407.1

Kaniewski, D., Marriner, N., Cheddadi, R., Morhange, C., Bretschneider, J., Jans, G., Otto, T., Luce, F., Van Campo, E., 2019. Cold and dry outbreaks in the eastern Mediterranean 3200 years ago. Geology 47, 933–937. https://doi.org/10.1130/g46491.1

Kaniewski, D., Paulissen, E., De Laet, V., Dossche, K., Waelkens, M., 2007. A high-resolution Late Holocene landscape ecological history inferred from an intramontane basin in the Western Taurus Mountains, Turkey. Quat. Sci. Rev. 26, 2201–2218. https://doi.org/10.1016/j.quascirev.2007.04.015

Kaniewski, D., Van Campo, E., Guiot, J., Le Burel, S., Otto, T., Baeteman, C., 2013. Environmental Roots of the Late Bronze Age Crisis. PLoS One 8, 1–10. https://doi.org/10.1371/journal.pone.0071004

Kaptijn, E., Poblome, J., Vanhaverbeke, H., Bakker, J., Waelkens, M., 2013. Societal changes in the Hellenistic, Roman and early Byzantine periods. Results from the Sagalassos Territorial Archaeological Survey 2008 (southwest Turkey). Anatol. Stud. 63, 75–95. https://doi.org/10.1017/S0066154613000057

Karaca, M., Deniz, A., Tayanç, M., 2000. Cyclone track variability over Turkey in association with regional climate. Int. J. Climatol. 20, 1225–1236. https://doi.org/10.1002/1097-0088(200008)20:10<1225::AID-JOC535>3.0.CO;2-1

Knapp, A.B., Manning, S.W., 2016. Crisis in Context: The End of the Late Bronze Age in the Eastern Mediterranean. Am. J. Archaeol. 120, 99–149. https://doi.org/10.3764/aja.120.1.0099

Koç, K., Koşun, E., Cheng, H., Demirtaş, F., Lawrence Edwards, R., Fleitmann, D., 2020. Black carbon traces of human activities in stalagmites from Turkey. J. Archaeol. Sci. 123, 105255. https://doi.org/10.1016/J.JAS.2020.105255

Kokkinia, C., 2000. Die Opramoas-Inschrift von Rhodiapolis: Euergetismus und Soziale Elite in Lykien. Rudolf Habelt, Bonn.

Kutiel, H., Benaroch, Y., 2002. North Sea-Caspian pattern (NCP) - An upper level atmospheric teleconnection affecting the Eastern Mediterranean: Identification and definition. Theor. Appl. Climatol. 71, 17–28. https://doi.org/10.1007/s704-002-8205-x

Kutiel, H., Maheras, P., Türkeş, M., Paz, S., 2002. North Sea - Caspian Pattern (NCP) - An upper level atmospheric teleconnection affecting the eastern Mediterranean - Implications on the regional climate. Theor. Appl. Climatol. https://doi.org/10.1007/s00704-002-0674-8

Kutiel, H., Türkeş, M., 2005. New evidence for the role of the North Sea - Caspian Pattern on the temperature and precipitation regimes in continental Central Turkey. Geogr. Ann. Ser. A Phys. Geogr. 87, 501–513. https://doi.org/10.1111/j.0435-3676.2005.00274.x

Kuzucuoğlu, C., Dörfler, W., Kunesch, S., Goupille, F., 2011. Mid- to late-Holocene climate change in central Turkey: The tecer lake record. Holocene 21, 173–188. https://doi.org/10.1177/0959683610384163

Lionello, P., 2012. The Climate of the Mediterranean Region: From the Past to the Future. Elsevier Inc., London.

Luterbacher, J., Garcia-Herrera, R., Akçer-Ön, S., Allan, R., Alvarez-Castro, M.C., Benito, G., Booth, J., Buntgen, U., Cagatay, N., Colombaroli, D., Davis, B., Esper, J., Felis, T., Fleitmann, D., Frank, D., Gallego, D., Garcia-Bustamante, E., Glaser, R., González-Rouco, J.F., Goosse, H., Kiefer, T., Macklin, M.G., Manning, S., Montagna, P., Newman, L., Power, M.J., Rath, V., Ribera, P., Riemann, D., Roberts, N., Sicre, M.A., Silenzi, S., Tinner, W., Valero-Garces, B., van der Schrier, G., Tzedakis, C., Vanniere, B., Vogt, S., Wanner, H., Werner, J.P., Willet, G., Williams, M.H., Xoplaki, E., Zerefos, C., Zorita, E., 2012. A review of 2000 years of paleoclimatic evidence in the Mediterranean, in: Lionello, P. (Ed.), The Climate of the Mediterranean Region: From the Past to the Future. Elsevier, Amsterdam, pp. 87–185.

Malalas, J., 2017. The Chronicle of John Malalas, The Chronicle of John Malalas. Australian Association for Byzantine Studies, Melbourne. https://doi.org/10.1163/9789004344600

Manning, S.W., Lorentzen, B., Welton, L., Batiuk, S., Harrison, T.P., 2020. Beyond megadrought and collapse in the Northern Levant: The chronology of Tell Tayinat and two historical inflection episodes, around 4.2ka BP, and following 3.2ka BP, PLoS ONE. https://doi.org/10.1371/journal.pone.0240799

Mannocchi, F., Todisco, F., Vergni, L., 2004. Agricultural drought: indices, definition and analysis, in: The Basis of Civilization-Water Science? (Proceedings of the UNESCO/IAIIS/IWIIA Symposium Held in Rome. December 2003). IAHS Publ, Rome.

Masson-Delmotte, V., Schulz, M., Abe-Ouchi, A., Beer, J., Ganopolski, A., Gonzalez-Rouco, J.F., Jansen, E., Lambeck, K., Luterbacher, J., Naish, T., Osborn, T., Otto-Bliesner, B., Quinn, T., Ramesh, R., Rojas, M., Shao, X., Timmerman, A., 2013. Information from Paleoclimate Archives, in: Stocker, T.F., Qin, D., Plattner, G.-K., Tignor, M., Allen, S.K., Boschung, J., Nauels, A., Xia, Y., Bex, V., Midgley, P.M. (Eds.), Climate Change 2013: The Physical Science Basis. Contribution of Working Group I to the Fifth Assessment Report of the Intergovernmental Panel on Climate Change. Cambridge University Press, Cambridge, pp. 383–464.

Mayewski, P.A., Rohling, E.E., Stager, J.C., Karlén, W., Maasch, K.A., Meeker, L.D., Meyerson, E.A., Gasse, F., van Kreveld, S., Holmgren, K., Lee-Thorp, J., Rosqvist, G., Rack, F., Staubwasser, M., Schneider, R.R., Steig, E.J., 2004. Holocene climate variability. Quat. Res. 62, 243–255. https://doi.org/10.1016/j.yqres.2004.07.001

McDermott, F., Schwarcz, H.P., Rowe, P.J., 2006. Isotopes in speleothems, in: Leng, M.J. (Ed.), Isotopes in Palaeoenvironmental Research. Springer, Dordrecht, The Netherlands, pp. 185–226.

McDonald, J., Drysdale, R., Hill, D., 2004. The 2002-2003 El Niño recorded in Australian cave drip waters: Implications for reconstructing rainfall histories using stalagmites. Geophys. Res. Lett. 31, 1–4. https://doi.org/10.1029/2004GL020859

Morin, E., Ryb, T., Gavrieli, I., Enzel, Y., 2019. Mean, variance, and trends of Levant precipitation over the past 4500 years from reconstructed Dead Sea levels and stochastic modeling. Quat. Res. (United States) 91, 751–767. https://doi.org/10.1017/qua.2018.98

Newfield, T.P., 2018. The Climate Downturn of 536-50, in: White, S., Pfister, C., Mauelshagen, F. (Eds.), The Palgrave Handbook of Climate History. Palgrave Macmillan, London, pp. 447–493. https://doi.org/10.1057/978-1-137-43020-5

Öztürk, M.Z., Çetınkaya, G., Aydin, S., 2017. Köppen-Geiger İklim Sınıflandırmasına Göre Türkiye’nin İklim Tipleri - (Climate Types of Turkey According to Köppen-Geiger Climate Classification). Istanbul Univ. J. Geogr. 35, 17–27. https://doi.org/10.26650/jgeog330955

Papadopoulos, G.A., Daskalaki, E., Fokaefs, A., Giraleas, N., 2007. Tsunami hazards in the Eastern Mediterranean: Strong earthquakes and tsunamis in the East Hellenic Arc and Trench system. Nat. Hazards Earth Syst. Sci. 7, 57–64. https://doi.org/10.5194/nhess-7-57-2007

Peel, M.C., Finlayson, B.L., McMahon, T.A., 2007. Updated world map of the Köppen-Geiger climate classification. Hydrol. Earth Syst. Sci. https://doi.org/10.5194/hess-11-1633-2007

Peterson, T.C., Vose, R.S., 1997. An Overview of the Global Historical Climatology Network Temperature Database. Bull. Am. Meteorol. Soc. 78, 2837–2849. https://doi.org/10.1175/1520-0477(1997)078<2837:AOOTGH>2.0.CO;2

Pirazzoli, P.A., Laborel, J., Stiros, S.C., 1996. Earthquake clustering in the eastern Mediterranean during historical times. J. Geophys. Res. Solid Earth 101, 6083–6097. https://doi.org/10.1029/95jb00914

Poblome, J., 2015. The Economy of the Roman World as a Complex Adaptive System: Testing the Case in Second to Fifth Century CE Sagalassos, in: Erdkamp, P., Verboven, K. (Eds.), Structure and Performance in the Roman Economy: Models, Methods, and Case Studies. Éditions Latomus, Brussels, pp. 97–140.

Psomiadis, D., Dotsika, E., Albanakis, K., Ghaleb, B., Hillaire-Marcel, C., 2018. Speleothem record of climatic changes in the northern Aegean region (Greece) from the Bronze Age to the collapse of the Roman Empire. Palaeogeogr. Palaeoclimatol. Palaeoecol. 489, 272–283. https://doi.org/10.1016/j.palaeo.2017.10.021

Rowe, P.J., Wickens, L.B., Sahy, D., Marca, A.D., Peckover, E., Noble, S., Özkul, M., Baykara, M.O., Millar, I.L., Andrews, J.E., 2020. Multi-proxy speleothem record of climate instability during the early last interglacial in southern Turkey. Palaeogeogr. Palaeoclimatol. Palaeoecol. 538, 109422. https://doi.org/10.1016/J.PALAEO.2019.109422

Sariş, F., Hannah, D.M., Eastwood, W.J., 2010. Spatial variability of precipitation regimes over Turkey. Hydrol. Sci. J. 55, 234–249. https://doi.org/10.1080/02626660903546142

Scholz, D., Hoffmann, D.L., 2011. StalAge - An algorithm designed for construction of speleothem age models. Quat. Geochronol. 6, 369–382. https://doi.org/10.1016/j.quageo.2011.02.002

Seguin, J., Avramidis, P., Dörfler, W., Emmanouilidis, A., Unkel, I., 2020. A 2600-year high-resolution climate record from Lake Trichonida (SW Greece). E&G Quat. Sci. J. 69, 139–160. https://doi.org/10.5194/egqsj-69-139-2020

Sezen, C., Partal, T., 2019. The impacts of Arctic oscillation and the North Sea Caspian pattern on the temperature and precipitation regime in Turkey. Meteorol. Atmos. Phys. 131, 1677–1696. https://doi.org/10.1007/s00703-019-00665-w

Sharifi, A., Pourmand, A., Canuel, E.A., Ferer-Tyler, E., Peterson, L.C., Aichner, B., Feakins, S.J., Daryaee, T., Djamali, M., Beni, A.N., Lahijani, H.A.K., Swart, P.K., 2015. Abrupt climate variability since the last deglaciation based on a high-resolution, multi-proxy peat record from NW Iran: The hand that rocked the Cradle of Civilization? Quat. Sci. Rev. 123, 215–230. https://doi.org/10.1016/j.quascirev.2015.07.006

Similox-Tohon, D., Sintubin, M., Muchez, P., Verhaert, G., Vanneste, K., Fernandez, M., Vandycke, S., Vanhaverbeke, H., Waelkens, M., 2006. The identification of an active fault by a multidisciplinary study at the archaeological site of Sagalassos (SW Turkey). Tectonophysics 420, 371–387. https://doi.org/10.1016/j.tecto.2006.03.026

Sinha, A., Kathayat, G., Weiss, H., Li, H., Cheng, H., Reuter, J., Schneider, A.W., Berkelhammer, M., Adalı, S.F., Stott, L.D., Lawrence Edwards, R., 2019. Role of climate in the rise and fall of the Neo-Assyrian Empire. Sci. Adv 5, 6656–6669.

Steinhilber, F., Beer, J., Fro, C., 2009. Total solar irradiance during the Holocene 36, 1–5. https://doi.org/10.1029/2009GL040142

Stiros, S.C., 2001. The AD 365 Cret earthquake and possible seismic clustering during the fourth to sixth centuries AD in the Eastern Mediterranean: A review of historical and archaeological data. J. Struct. Geol. 23, 545–562. https://doi.org/10.1016/S0191-8141(00)00118-8

Talloen, P., 2015. Cult in Pisidia. Religious Practice in Southwestern Asia Minor from Alexander the Great to the Rise of Christianity. (Studies in Eastern Mediterranean Archaeology, 10). Brepols, Turnhout.

Tan, O., Tapirdamaz, M.C., Yörük, A., 2008. The earthquake catalogues for Turkey. Turkish J. Earth Sci. 17, 405–418.

Tanner, S.D., Baranov, V.I., Bandura, D.R., 2002. Reaction cells and collision cells for ICP-MS: A tutorial review. Spectrochim. Acta - Part B At. Spectrosc. 57, 1361–1452. https://doi.org/10.1016/S0584-8547(02)00069-1

Treble, P., Shelley, J.M.G., Chappell, J., 2003. Comparison of high resolution sub-annual records of trace elements in a modern (1911-1992) speleothem with instrumental climate data from southwest Australia. Earth Planet. Sci. Lett. 216, 141–153. https://doi.org/10.1016/S0012-821X(03)00504-1

Tremaine, D.M., Froelich, P.N., 2013. Speleothem trace element signatures: A hydrologic geochemical study of modern cave dripwaters and farmed calcite. Geochim. Cosmochim. Acta 121, 522–545. https://doi.org/10.1016/j.gca.2013.07.026

Tudryn, A., Tucholka, P., Özgûr, N., Gibert, E., Elitok, O., Kamaci, Z., Massault, M., Poisson, A., Platevoet, B., 2013. A 2300-year record of environmental change from SW Anatolia, Lake Burdur, Turkey. J. Paleolimnol. 49, 647–662. https://doi.org/10.1007/s10933-013-9682-1

Türkeş, M., Erlat, E., 2009. Winter mean temperature variability in Turkey associated with the North Atlantic Oscillation. Meteorol. Atmos. Phys. 105, 211–225. https://doi.org/10.1007/s00703-009-0046-3

Türkeş, M., Erlat, E., 2003. Precipitation changes and variability in Turkey linked to the North Atlantic oscillation during the period 1930-2000. Int. J. Climatol. 23, 1771–1796. https://doi.org/10.1002/joc.962

Ulbrich, U., Lionello, P., Belušić, D., Jacobeit, J., Knippertz, P., Kuglitsch, G., Leckebusch, G.C., Luterbacher, J., Maugeri, M., Maheras, P., Nissen, K.M., Pavan, V., Pinto, J.G., Saaroni, H., Seubert, S., Toreti, A., Xoplaki, E., Ziv, B., 2012. Climate of the Mediterranean: Synoptic Patterns, Temperature, Precipitation, Winds and their Extremes, in: Lionello, P. (Ed.), The Climate of the Mediterranean Region: From the Past to the Future. Elsevier, Amsterdam, pp. 301–346.

Ülgen, U.B., Franz, S.O., Biltekin, D., Çagatay, M.N., Roeser, P.A., Doner, L., Thein, J., 2012. Climatic and environmental evolution of Lake Iznik (NW Turkey) over the last ∼4700 years. Quat. Int. 274, 88–101. https://doi.org/10.1016/j.quaint.2012.06.016

Ünal-İmer, E., Shulmeister, J., Zhao, J.-X., Uysal, I.T., Feng, Y.-X., Nguyen, A.D., Yüce, G., 2015. An 80 kyr-long continuous speleothem record from Dim Cave, SW Turkey with paleoclimatic implications for the Eastern Mediterranean. Sci. Reports 2015 51 5, 1–11. https://doi.org/10.1038/srep13560

Ünal-İmer, E., Shulmeister, J., Zhao, J.X., Uysal, I.T., Feng, Y.X., 2016. High-resolution trace element and stable/radiogenic isotope profiles of late Pleistocene to Holocene speleothems from Dim Cave, SW Turkey. Palaeogeogr. Palaeoclimatol. Palaeoecol. 452, 68–79. https://doi.org/10.1016/j.palaeo.2016.04.015

Unal, Y.S., Deniz, A., Toros, H., Incecik, S., 2012. Temporal and spatial patterns of precipitation variability for annual, wet, and dry seasons in Turkey. Int. J. Climatol. 32, 392–405. https://doi.org/10.1002/joc.2274

University of East Anglia Climatic Research Unit, Harris, I.C., Jones, P.D., Osborn, T., 2020. CRU TS4.04: Climatic Research Unit (CRU) Time-Series (TS) version 4.04 of high-resolution gridded data of month-by-month variation in climate (Jan. 1901- Dec. 2019). Norwich.

Van Geel, B., Coope, G.R., Van Der Hammen, T., 1989. Palaeoecology and stratigraphy of the lateglacial type section at Usselo (the Netherlands). Rev. Palaeobot. Palynol. 60. https://doi.org/10.1016/0034-6667(89)90072-9

Vandam, R., Kaptijn, E., Broothaerts, N., De Cupere, B., Marinova, E., Van Loo, M., Verstraeten, G., Poblome, J., 2019. “Marginal” Landscapes: Human Activity, Vulnerability, and Resilience in the Western Taurus Mountains (Southwest Turkey). J. East. Mediterr. Archaeol. Herit. Stud. 7, 432–450. https://doi.org/doi: 10.5325/jeasmedarcherstu.7.4.0432

Vermoere, M., Bottema, S., Vanhecke, L., Waelkens, M., Paulissen, E., Smets, E., 2002. Palynological evidence for late-Holocene human occupation recorded in two wetlands in SW Turkey. The Holocene 12, 569–584. https://doi.org/10.1191/0959683602hl568rp

Vicente-Serrano, S.M., Beguería, S., López-Moreno, J.I., 2010. A multiscalar drought index sensitive to global warming: The standardized precipitation evapotranspiration index. J. Clim. 23, 1696–1718. https://doi.org/10.1175/2009JCLI2909.1

Waelkens, M., Sintubin, M., Muchez, P., Paulissen, E., 2000. Archaeological, geomorphological and geological evidence for a major earthquake at Sagalassos (SW Turkey) around the middle of the seventh century AD. Geol. Soc. Spec. Publ. 171, 373–383. https://doi.org/10.1144/GSL.SP.2000.171.01.27

Wanner, H., Wanner, H., Mercolli, L., Mercolli, L., Grosjean, M., Grosjean, M., Ritz, S.P., 2015. Holocene climate variability and change; a data-based review. J. Geol. Soc. London. 172, 254–263. https://doi.org/10.1144/jgs2013-101

Wassenburg, J.A., Riechelmann, S., Schröder-Ritzrau, A., Riechelmann, D.F.C., Richter, D.K., Immenhauser, A., Terente, M., Constantin, S., Hachenberg, A., Hansen, M., Scholz, D., 2020. Calcite Mg and Sr partition coefficients in cave environments: Implications for interpreting prior calcite precipitation in speleothems. Geochim. Cosmochim. Acta 269, 581–596. https://doi.org/10.1016/j.gca.2019.11.011

Woodbridge, J., Roberts, C.N., Palmisano, A., Bevan, A., Shennan, S., Fyfe, R., Eastwood, W.J., Izdebski, A., Çakırlar, C., Woldring, H., Broothaerts, N., Kaniewski, D., Finné, M., Labuhn, I., 2019. Pollen-inferred regional vegetation patterns and demographic change in Southern Anatolia through the Holocene. Holocene 29, 728–741. https://doi.org/10.1177/0959683619826635

Xoplaki, E., Luterbacher, J., Wagner, S., Zorita, E., Fleitmann, D., Preiser-Kapeller, J., Sargent, A.M., White, S., Toreti, A., Haldon, J.F., Mordechai, L., Bozkurt, D., Akçer-Ön, S., Izdebski, A., 2018. Modelling Climate and Societal Resilience in the Eastern Mediterranean in the Last Millennium. Hum. Ecol. 46, 363–379. https://doi.org/10.1007/s10745-018-9995-9

Figure 1.

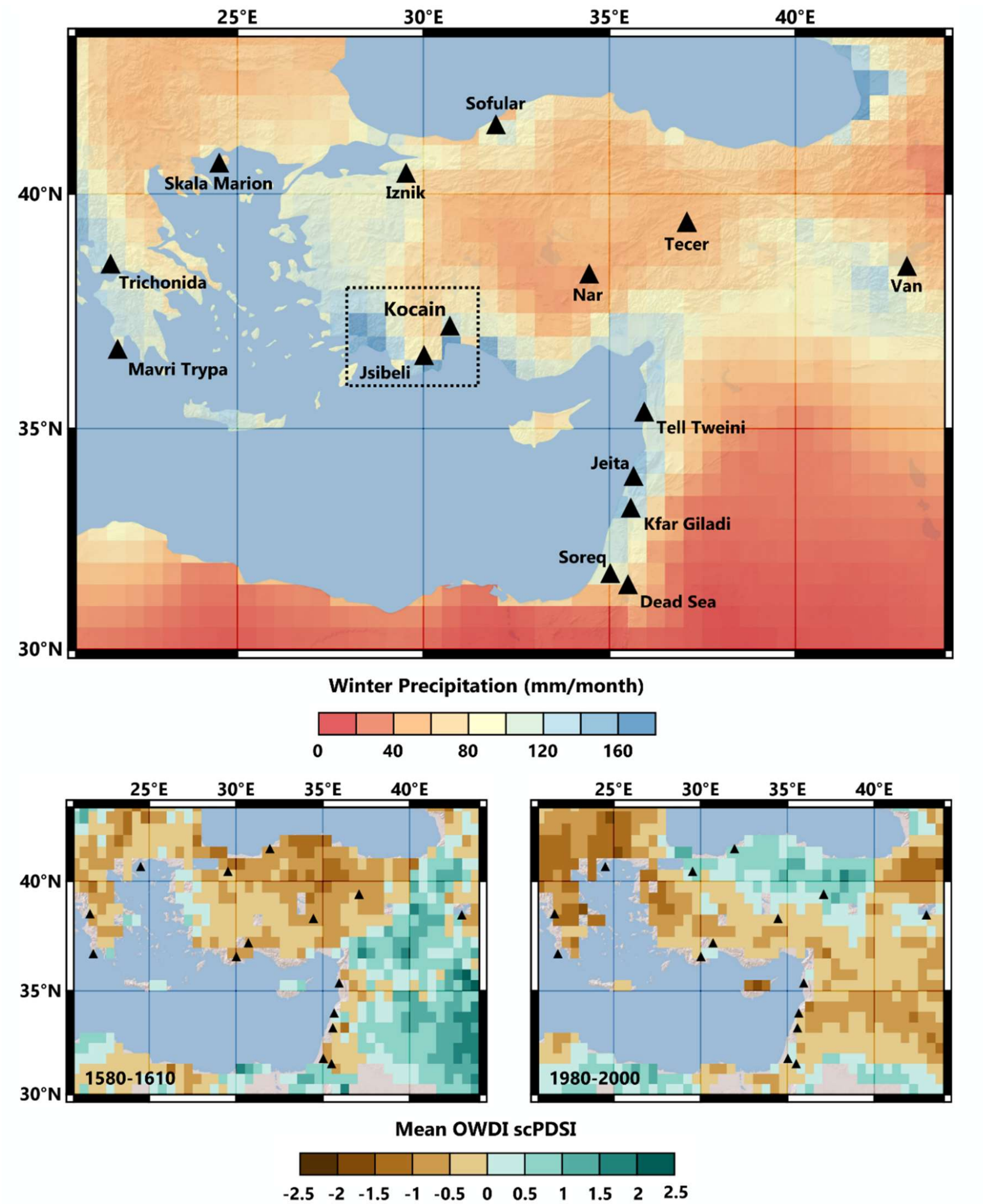
25°E
30°E
35°E
40°E
40°N
35°N
30°N
Sofular
Skala Marion
Iznik
Tecer
Trichonida
Nar
Van
Kocain
Mavri Trypa
Jsibeli
Tell Tweini
Jeita
Kfar Giladi
Soreq
Dead Sea
Winter Precipitation (mm/month)
0
40
80
120
160
1580-1610
1980-2000
Mean OWDI scPDSI
-2.5
-2
-1.5
-1
-0.5
0
0.5
1
1.5
2
2.5

Figure 2.

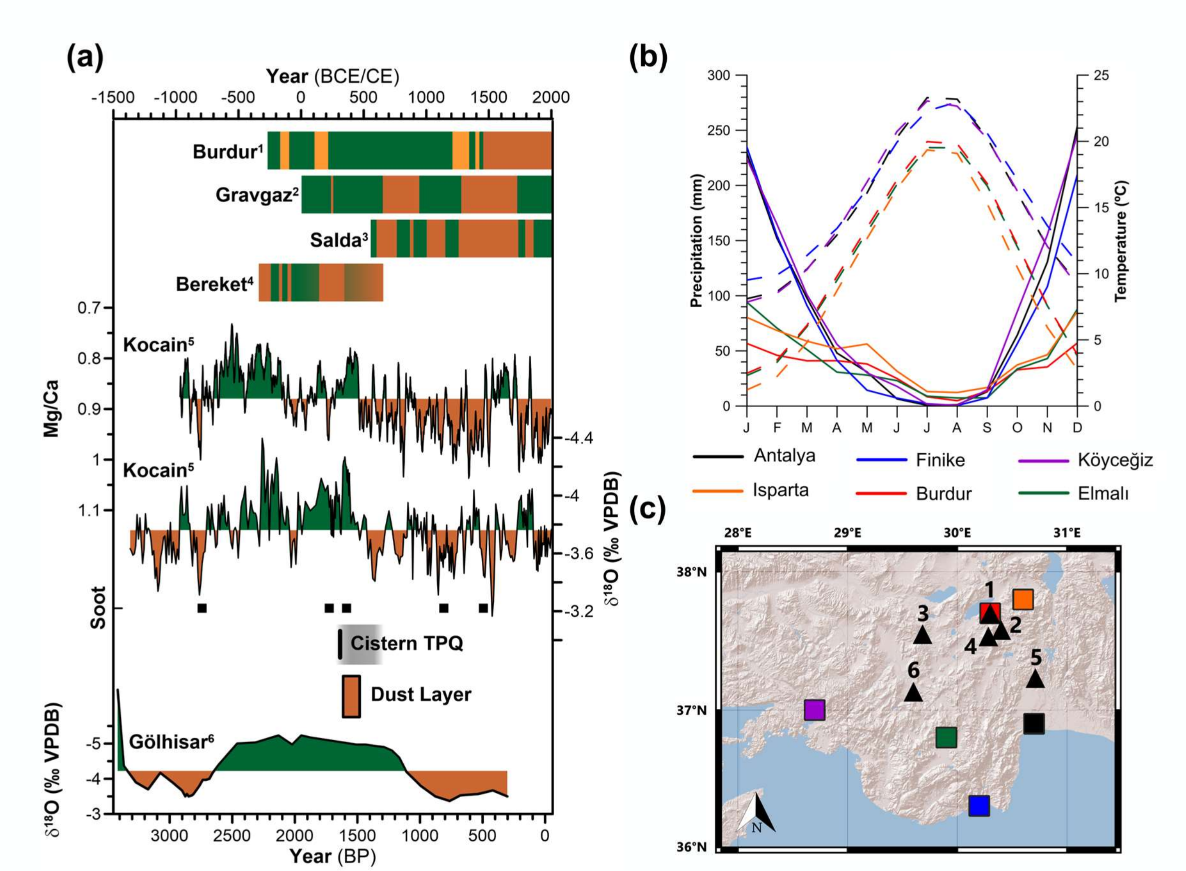
(a)
Year (BCE/CE)
-1500 -1000 -500 0 500 1000 1500 2000
Burdur1
Gravgaz2
Salda3
Bereket4
Kocain5
Mg/Ca
0.7 0.8 0.9 1 1.1
Kocain5
-4.4 -4 -3.6 -3.2
δ18O (‰ VPDB)
Soot
Cistern TPQ
Dust Layer
Gölhisar6
δ18O (‰ VPDB)
-5 -4 -3
3000 2500 2000 1500 1000 500 0
Year (BP)
(b)
Precipitation (mm)
Temperature (ºC)
J F M A M J J A S O N D
Antalya
Finike
Köyceğiz
Isparta
Burdur
Elmalı
(c)
28°E 29°E 30°E 31°E
38°N 37°N 36°N
1 2 3 4 5 6
N

Figure 3.

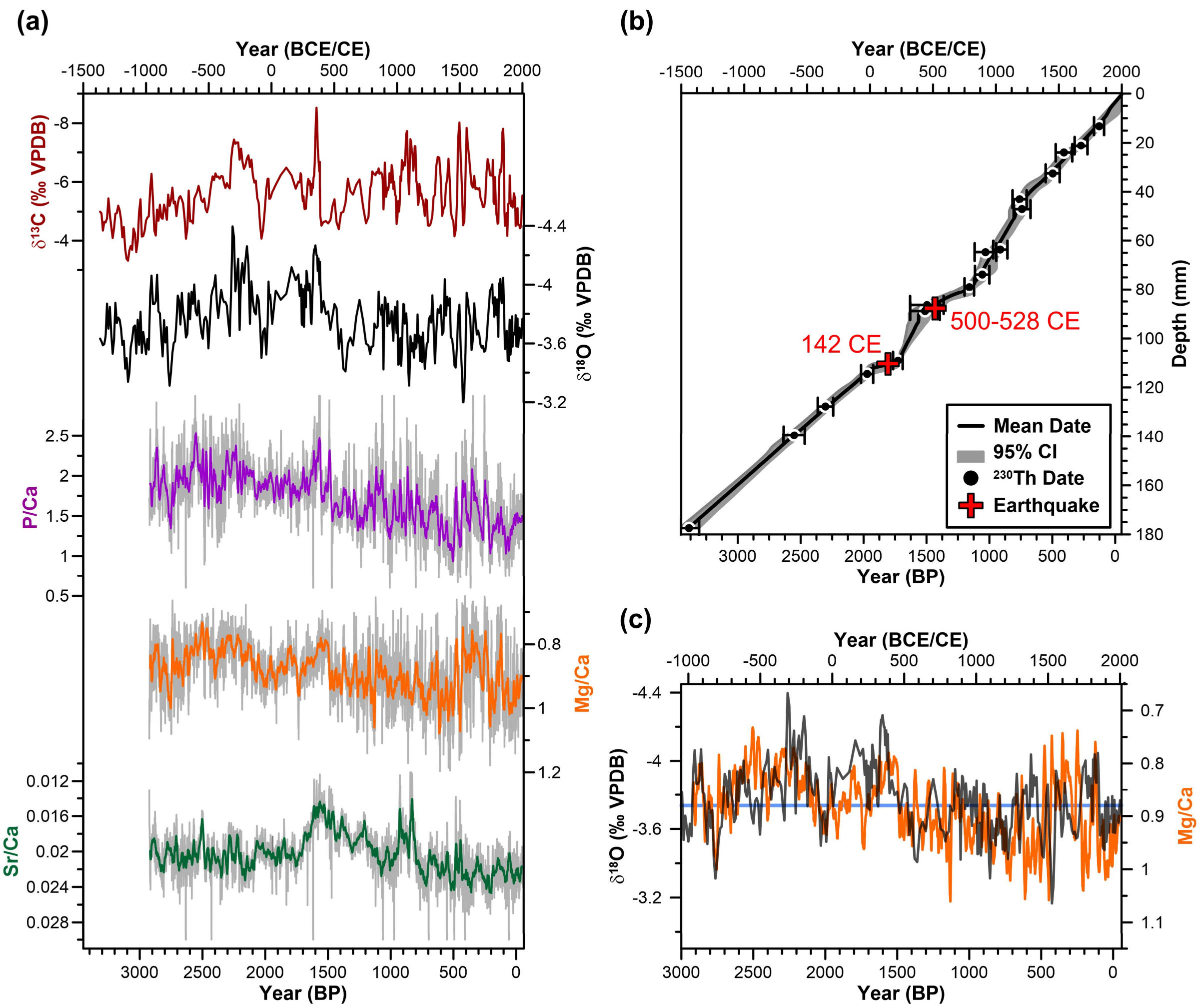
(a)
Year (BCE/CE)
δ13C (‰ VPDB)
δ18O (‰ VPDB)
P/Ca
Mg/Ca
Sr/Ca
Year (BP)
(b)
Year (BCE/CE)
Depth (mm)
500-528 CE
142 CE
Mean Date
95% CI
230Th Date
Earthquake
Year (BP)
(c)
Year (BCE/CE)
δ18O (‰ VPDB)
Mg/Ca
Year (BP)

Figure 4.

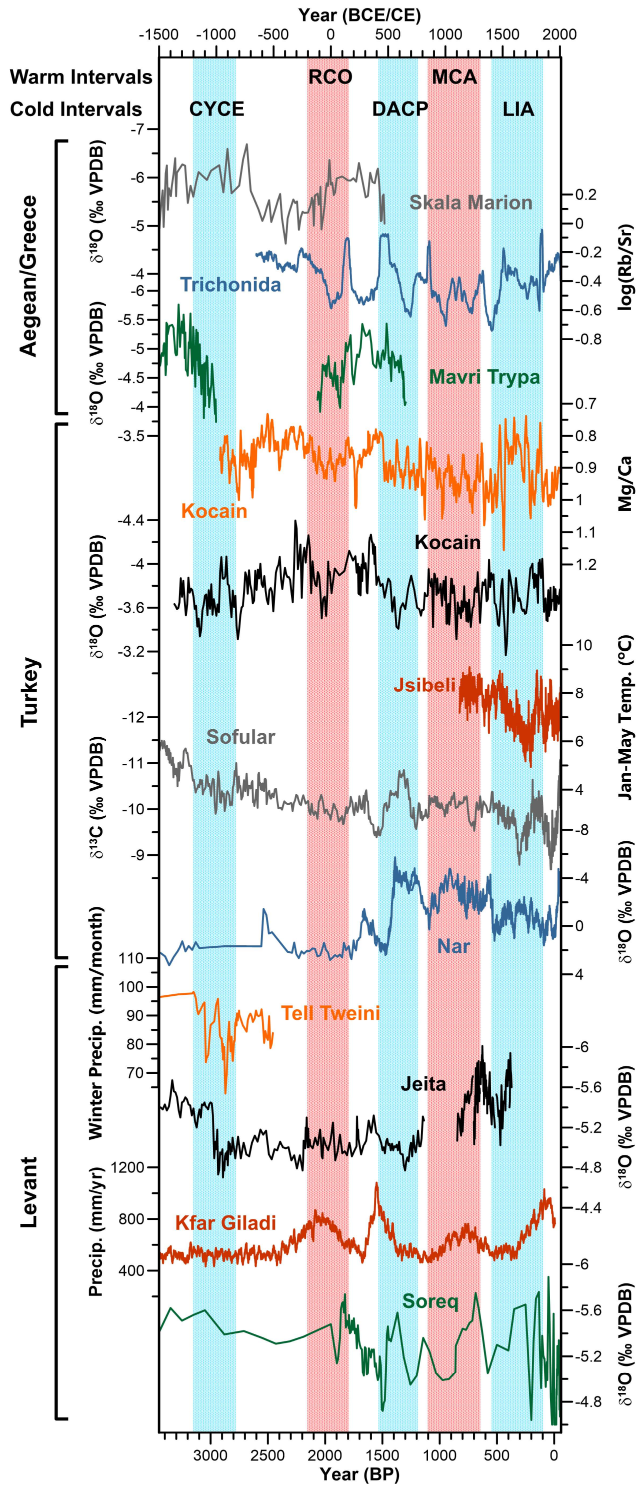
Year (BCE/CE)
Warm Intervals
Cold Intervals
CYCE
RCO
DACP
MCA
LIA
Aegean/Greece
Turkey
Levant
Skala Marion
Trichonida
Mavri Trypa
Kocain
Kocain
Jsibeli
Sofular
Nar
Tell Tweini
Jeita
Kfar Giladi
Soreq
δ18O (‰ VPDB)
δ13C (‰ VPDB)
log(Rb/Sr)
Mg/Ca
Jan-May Temp. (°C)
Winter Precip. (mm/month)
Precip. (mm/yr)
Year (BP)